

High-temperature in situ structural investigation on lead feldspar

PIERA BENNA,^{1,2,*} MARIO TRIBAUDINO,¹ AND EMILIANO BRUNO^{1,2}

¹Dipartimento di Scienze Mineralogiche e Petrologiche, Via Valperga Caluso 35, I-10125 Torino, Italy

²Centro di Studi sulla Geodinamica delle Catene Collisionali (C.N.R.), Via Accademia delle Scienze 5, I-10123 Torino, Italy

ABSTRACT

Single-crystal X-ray diffraction was performed in situ at $T = 20, 230, 465,$ and $700\text{ }^{\circ}\text{C}$ on a partially ordered lead feldspar ($\text{PbAl}_2\text{Si}_2\text{O}_8$, $I2/c$, $a = 8.402, b = 13.043, c = 14.308\text{ }\text{\AA}$, $\beta = 115.30^{\circ}$, $V = 1417.6\text{ }\text{\AA}^3$; $Q_{\text{od}} = 0.71$). The unit-cell expansion ($1.26 \times 10^{-5}\text{ }^{\circ}\text{C}^{-1}$) is close to that observed for other feldspars, sanidine in particular, and occurs predominantly along a^* . The electron-density at the Pb site evolves with temperature toward a bean-like configuration close to that observed in disordered lead feldspar. The average Pb position approaches the c -glide plane with increasing temperature. Consequently the intensity of the b -type reflections reduces dramatically without evidence of an increase of Al-Si disorder. The evolution of atomic displacement parameters of the Pb atom with temperature supports the view that at room temperature Pb shows considerable positional disorder. Dark-field in situ TEM observations show that b antiphase domains (APD) persist unchanged in shape and size up to $T = 690\text{ }^{\circ}\text{C}$. No diffuse component appears in b -type reflections in SAD patterns up to $935\text{ }^{\circ}\text{C}$, showing that the above changes in the Pb configuration do not affect the APD. The results suggest that, at $T > 700\text{ }^{\circ}\text{C}$, Pb reaches the glide plane assuming a configuration that may favor the Al-Si disorder.

INTRODUCTION

Data on thermal expansion and on phase transitions with temperature are available on many natural and synthetic feldspars (reviewed by Ribbe 1994), although full structural determinations from in situ single-crystal data collection are less common. High temperature (HT) structural investigations were done on high and low albite to determine the presence of positional disorder of sodium (Prewitt et al. 1976; Winter et al. 1977) and in anorthite to clarify the average configurations of the framework and the calcium after the $P\bar{1}-I\bar{1}$ phase transition (Czank 1973; Foit and Peacor 1973; Ghose et al. 1993). HT investigations on sanidine were also performed by Ohashi and Finger (1974, 1975) and most recently by Kimata et al. (1996). No data are presently available on the HT structures of feldspars other than the calcium, sodium, and potassium end-members. In particular the thermal behavior of $I2/c$ configurations in feldspars with an Al:Si ratio of 1:1 is unknown.

Recent investigations revealed that Al-Si ordering behavior is significantly different in lead feldspar ($\text{PbAl}_2\text{Si}_2\text{O}_8$) than in anorthite ($\text{CaAl}_2\text{Si}_2\text{Si}_2\text{O}_8$). Anorthite retains an ordered Al-Si configuration up to a temperature close to the melting point ($t_m = 1555\text{ }^{\circ}\text{C}$) and only limited changes in Al-Si ordering can be achieved by extreme heating (Benna et al. 1985; Carpenter 1992). A T_c of about $2100\text{ }^{\circ}\text{C}$ was estimated for the $I\bar{1}-C\bar{1}$ phase transition induced by Al-Si disordering in anorthite. Conse-

quently, the full Al-Si disorder can be obtained only at temperatures that are beyond melting and therefore the $I\bar{1}-C\bar{1}$ transition cannot be achieved experimentally.

Lead feldspar was synthesized both in ordered ($I2/c$) and in disordered ($C2/m$) configurations (Benna et al. 1996). The transition from the ordered to the disordered configuration can be experimentally bracketed at $T_c \approx 1180\text{ }^{\circ}\text{C}$, and the evolution of the order parameter Q_{od} with thermal treatment could be retrieved (Tribaudino et al. 1998). The observed transition temperature is lower than in anorthite and in strontium feldspar (Benna et al. 1995); the obvious suggestion is that the difference relies in the behavior of the non-tetrahedral cation. As a consequence, in lead feldspar a completely disordered Al-Si configuration ($Q_{\text{od}} \approx 0$) was achieved at temperatures significantly below melting. A similar occurrence was established by Malcherek et al. (1995) in $\text{BaAl}_2\text{Ge}_2\text{O}_8$ feldspar, showing as well a similar evolution in the equilibrium Q_{od} vs. T plot, although at higher temperatures ($T_c = 1417\text{ }^{\circ}\text{C}$). Room-temperature data indicate that thermal treatment of lead feldspar induces, together with the changes in Al-Si order, a significant evolution in the electron-density distribution and a remarkable shift of the average position of the Pb site. With increasing Al-Si disorder the electron density map near the Pb site becomes blurred and the average Pb position moves toward the c plane. Significant changes in Al-Si order could be obtained in air only after heating at $T > 850\text{ }^{\circ}\text{C}$. However the Pb position and the electron-density distribution are also expected to vary at lower temperatures as the movement of

* E-mail: benna@dsmpl.unito.it

TABLE 1. Single-crystal data at different temperatures (esd in brackets)

T (°C)	20	230	465	700
a (Å)	8.402(1)	8.422(2)	8.440(2)	8.448(2)
b (Å)	13.043(2)	13.045(3)	13.051(3)	13.057(2)
c (Å)	14.308(2)	14.310(4)	14.325(4)	14.332(3)
β (°)	115.30(1)	115.34(1)	115.33(2)	115.25(1)
V (Å ³)	1417.6	1420.9	1426.2	1429.8
μ (mm ⁻¹)	24.40	24.34	24.25	24.19
Refl. measured	6513	6502	6511	6509
Unique refl.	2934	2947	2953	2945
Refl. observed $F_o \geq 4\sigma(F_o)$	2092	1573	1365	1157
Refl. b type	814	474	319	241
No. refl. b /No. refl. a	0.637	0.431	0.305	0.263
$\Sigma F_{o(b)}/\Sigma F_{o(a)}$ $F_o \geq 2\sigma(F_o)$	0.065	0.033	0.022	0.018
R	0.050	0.062	0.063	0.067
wR^2	0.107	0.126	0.123	0.172
Goodness of fit	1.22	0.98	1.27	1.09

Note: $w = 1/[\sigma^2(F_o^2) + 0.1P^2]$, where $P = (F_o^2 + 2F_c^2)/3$.

the Pb atom reflects the relaxation of the structure toward a configuration favored by the existing constant Al-Si configuration. This would not induce a variation in Al-Si ordering, which is kinetically inhibited at low temperature, but may indicate an evolution of the Pb configuration at constant Q_{ad} . An investigation on this evolution may give some information on the role played by the non-tetrahedral cation during disordering in lead feldspar.

Furthermore, the large and asymmetric electron-density distribution found at the Pb site in lead feldspar could arise either from the large thermal motion of a single Pb atom or by positional disorder on more than one Pb site. The evolution of the atomic displacement parameters with temperature should indicate in the case of positional disorder the presence of a significant residual at $T = 0$ K, in the same manner as previously observed for high albite (Prewitt et al. 1976).

A single-crystal in situ XRD study was therefore performed at $T < 850$ °C to clarify the evolution of the structural configurations of Pb and framework with temperature and to elucidate the presence of positional disorder in the Pb configuration. The HT behavior of lead feldspar was compared with that of other feldspars both as concerns the unit-cell expansion and the structural details. TEM investigation was also carried out, to clarify the effect of the evolution of the Pb configuration with temperature on the size and shape of b antiphase domains.

EXPERIMENTAL METHODS

The sample was synthesized by slow cooling from a melt, with subsequent annealing at $T = 950$ °C for 192 h. As in Benna et al. (1996), a mixture of oxides was used as starting material, with slight excess in PbO to compensate the loss in Pb during melting and cooling from HT. The crystal chosen for data collection (0.15 mm \times 0.05 mm \times 0.04 mm) was fixed to a quartz glass fiber by GA-100 HT cement (Micro-Measurements Division, Raleigh, North Carolina). The intensities were collected

with a Siemens P4 four-circle diffractometer, using graphite-monochromatized MoK α radiation ($\lambda = 0.71073$ Å), and the θ - 2θ scan-type technique. An A.E.T. thermal attachment (Pt-PtRh 10% thermocouple) was employed for the HT XRD (Argoud and Capponi 1984), with a stream of hot N₂. The same set of 30 reflections was used at the different temperatures for cell parameter refinements. The reciprocal lattice sphere was explored up to $2\theta = 70$ ° and two sets of equivalent reflections were measured ($h \pm k \pm l$) at variable scanning speed (2–15 °C/min). The heating attachment prevented measurements for application of the empirical absorption correction at HT. An empirical absorption correction based on the ψ -scan method (North et al. 1968) was performed for the room temperature measurement and applied also for higher temperatures. The data were corrected for background and Lorentz-polarization effect using the SHELXTL-Plus 1990 system. A weighting scheme was used for the data at the end of the refinement cycles. In all the refinements a ($h + k = 2n$, $l = 2n$) and b -type ($h + k = 2n + 1$, $l = 2n + 1$) reflections were found and the presence of a $I2/c$ space group was assumed. Reflections with $F_o \geq 4\sigma(F_o)$ were regarded as observed and used for the 25, 230, and 465 °C refinements. In the refinement at 700 °C, to cope with the low number of b observed reflections, all data were used. The refinements were carried out according to the procedure outlined in Tribaudino et al. (1998); a “split-atom model” for the Pb site was used in all the refinements, and an average single-Pb refinement (“non-split model”) was done at the end of the split Pb cycles, fixing the framework atoms.

In situ HT TEM investigations were performed on a powdered sample, crushed in agate mortar, and dispersed on a holey carbon film, using a Philips CM12 electron microscope operating at 120 kV and equipped with a Gatan 652 double tilt heating stage.

Unit-cell parameters, refinement data, atomic fractional coordinates, and displacement parameters are given in Tables 1 and 2, and the relevant bond lengths are reported

TABLE 2. Atomic fractional coordinates ($\times 10^4$), site occupation factors (s.o.f.), equivalent isotropic,* and anisotropic† displacement coefficients ($\text{\AA}^2 \times 10^3$)

Site	x	y	z	s.o.f.	U_{eq}	U_{11}	U_{22}	U_{33}	U_{12}	U_{13}	U_{23}
T = 20 °C											
Pb	2709(1)	-80(1)	723(1)		33(0)	12(0)	55(0)	28(0)	-4(0)	5(0)	-2(0)
Pb'	2698(2)	-113(2)	730(1)	0.74	26(0)	12(0)	40(1)	23(1)	-8(0)	5(0)	-1(0)
Pb''	2768(10)	103(18)	687(6)	0.26	47(2)	11(1)	80(6)	47(2)	9(2)	8(1)	4(2)
T ₁ (0)	62(3)	1767(1)	1097(2)		11(0)	9(1)	13(1)	10(1)	-2(1)	4(1)	-0(0)
T ₁ (z)	33(3)	1794(2)	6156(2)		8(0)	5(1)	12(1)	7(1)	-2(1)	1(1)	-0(1)
T ₂ (0)	6950(3)	1192(2)	1717(2)		8(0)	4(1)	9(1)	8(1)	0(1)	0(1)	0(1)
T ₂ (z)	6883(3)	1147(1)	6739(2)		9(0)	6(1)	10(1)	12(1)	-0(1)	4(1)	-1(1)
O _A (1)	41(10)	1342(5)	12(5)		16(1)	18(2)	24(3)	6(2)	-3(2)	5(2)	-0(2)
O _A (2)	5986(7)	-11(4)	1470(1)		14(1)	8(2)	10(2)	20(2)	-1(2)	1(2)	0(2)
O _B (0)	8248(9)	1297(5)	1074(5)		19(1)	11(3)	22(3)	24(3)	-3(2)	8(2)	0(2)
O _B (z)	8144(10)	1311(5)	6170(6)		22(1)	17(3)	25(3)	29(4)	-5(2)	13(3)	1(2)
O _C (0)	178(9)	3006(5)	1224(5)		18(1)	12(3)	22(3)	20(3)	-5(2)	5(3)	-3(2)
O _C (z)	183(10)	3103(4)	6323(5)		19(1)	21(3)	15(2)	18(3)	-9(2)	5(3)	-3(2)
O _D (0)	1857(9)	1240(5)	1969(5)		19(1)	13(3)	26(3)	11(3)	1(2)	-1(2)	2(2)
O _D (z)	1987(9)	1212(4)	7010(5)		18(1)	14(3)	21(3)	13(3)	-2(2)	0(2)	3(2)
T = 230 °C											
Pb	2731(1)	-63(1)	713(1)		51(0)	21(0)	84(1)	44(0)	-6(1)	8(0)	-4(1)
Pb'	2705(5)	-136(4)	726(3)	0.59	38(1)	21(1)	54(1)	34(1)	-13(1)	7(1)	-1(1)
Pb''	2787(9)	89(13)	686(6)	0.41	55(2)	19(1)	81(5)	61(2)	6(2)	12(1)	5(2)
T ₁ (0)	59(5)	1777(2)	1100(3)		16(1)	16(2)	19(1)	12(2)	-4(1)	5(1)	1(1)
T ₁ (z)	39(5)	1798(2)	6158(3)		14(1)	11(2)	17(2)	13(2)	-3(1)	5(2)	1(1)
T ₂ (0)	6959(6)	1194(3)	1714(3)		15(1)	13(2)	13(2)	15(2)	2(1)	2(2)	2(1)
T ₂ (z)	6901(5)	1148(2)	6732(3)		15(1)	8(1)	18(1)	15(2)	-3(1)	3(1)	-3(1)
O _A (1)	41(18)	1342(6)	11(8)		25(2)	29(4)	31(4)	14(3)	-1(4)	9(3)	-1(4)
O _A (2)	6023(9)	-16(6)	1462(6)		24(2)	11(3)	16(3)	38(4)	0(3)	4(3)	-1(4)
O _B (0)	8236(13)	1310(8)	1078(8)		28(2)	17(5)	37(5)	29(5)	-8(4)	8(4)	1(4)
O _B (z)	8153(16)	1320(8)	6159(10)		37(3)	31(7)	39(6)	52(8)	-7(4)	28(6)	1(5)
O _C (0)	200(13)	3011(7)	1217(8)		25(2)	20(5)	32(5)	26(5)	-8(4)	12(4)	-2(3)
O _C (z)	176(15)	3101(7)	6332(9)		30(2)	26(6)	27(5)	36(6)	-10(4)	11(5)	-6(4)
O _D (0)	1815(16)	1252(8)	1976(8)		31(2)	28(6)	37(5)	22(5)	4(4)	5(5)	-1(4)
O _D (z)	1982(13)	1208(7)	7011(7)		23(2)	12(4)	35(5)	16(4)	-1(3)	-2(4)	5(3)
T = 465 °C											
Pb	2745(1)	-50(1)	706(1)		65(0)	26(0)	104(1)	56(0)	-9(1)	11(0)	-7(1)
Pb'	2703(8)	-157(6)	717(4)	0.44	45(1)	24(1)	63(2)	43(2)	-21(1)	10(1)	-5(1)
Pb''	2798(8)	68(11)	693(4)	0.56	67(2)	26(1)	98(4)	71(2)	4(2)	13(1)	-0(2)
T ₁ (0)	61(6)	1786(3)	1095(3)		21(1)	24(3)	24(2)	19(2)	-4(1)	12(2)	-0(1)
T ₁ (z)	39(6)	1802(3)	6160(3)		15(1)	11(2)	18(2)	14(2)	-6(1)	3(2)	-1(1)
T ₂ (0)	6980(5)	1194(3)	1727(3)		15(1)	6(2)	18(2)	17(2)	1(1)	1(2)	2(1)
T ₂ (z)	6890(7)	1152(3)	6726(3)		20(1)	19(2)	19(2)	24(2)	-5(1)	10(2)	-5(1)
O _A (1)	28(20)	1347(7)	9(9)		30(2)	34(4)	41(4)	15(3)	1(6)	11(3)	-7(5)
O _A (2)	6037(9)	-12(7)	1468(6)		30(2)	18(3)	19(3)	46(4)	15(5)	8(3)	0(5)
O _B (0)	8287(18)	1308(8)	1100(9)		38(3)	36(8)	43(6)	41(7)	-12(5)	20(6)	-7(4)
O _B (z)	8128(17)	1329(9)	6134(10)		43(3)	22(6)	51(6)	62(9)	-10(5)	24(6)	8(5)
O _C (0)	138(15)	3023(7)	1207(8)		30(2)	24(6)	40(5)	27(5)	-5(4)	10(4)	-10(4)
O _C (z)	265(17)	3096(7)	6356(10)		40(3)	34(7)	20(4)	58(7)	-19(4)	12(6)	-6(4)
O _D (0)	1789(19)	1261(9)	1969(9)		44(3)	42(8)	48(6)	36(7)	15(6)	10(6)	-2(5)
O _D (z)	1983(14)	1217(7)	7015(7)		28(2)	13(4)	46(5)	16(4)	-2(4)	-3(4)	8(4)
T = 700 °C											
Pb	2759(1)	-37(1)	702(1)		84(0)	38(0)	129(1)	76(0)	-4(1)	16(0)	-6(1)
Pb'	2751(8)	-170(4)	728(6)	0.5	65(1)	40(1)	80(2)	69(1)	-19(2)	19(1)	-1(2)
Pb''	2791(8)	120(4)	673(6)	0.5	77(1)	37(2)	99(3)	82(2)	10(2)	13(1)	7(2)
T ₁ (0)	72(5)	1788(2)	1098(3)		30(1)	29(2)	31(1)	29(2)	-4(1)	11(2)	1(1)
T ₁ (z)	29(5)	1808(2)	6156(3)		26(1)	23(2)	28(2)	27(2)	-5(1)	10(2)	-1(1)
T ₂ (0)	6985(5)	1194(3)	1728(3)		27(1)	18(2)	27(2)	32(2)	-4(1)	7(2)	-1(1)
T ₂ (z)	6914(4)	1155(2)	6725(2)		28(1)	23(2)	26(1)	33(2)	1(1)	10(2)	-1(1)
O _A (1)	22(17)	1354(6)	-1(8)		43(2)	51(4)	53(4)	31(3)	-11(5)	23(3)	-10(5)
O _A (2)	6060(9)	-20(6)	1459(6)		43(2)	32(3)	22(3)	68(5)	-3(4)	14(3)	-8(4)
O _B (0)	8274(14)	1336(7)	1107(8)		48(2)	39(6)	54(6)	47(6)	-10(4)	14(5)	-4(4)
O _B (z)	8141(16)	1334(9)	6138(10)		64(3)	40(6)	78(7)	84(9)	-18(5)	37(7)	3(6)
O _C (0)	186(13)	3024(7)	1220(7)		43(2)	37(6)	47(5)	49(5)	-16(4)	21(5)	-11(4)
O _C (z)	243(14)	3119(6)	6343(9)		54(3)	42(6)	28(4)	81(8)	-9(4)	16(6)	-5(4)
O _D (0)	1811(16)	1269(8)	1968(8)		56(3)	59(8)	60(6)	40(5)	14(5)	14(6)	6(5)
O _D (z)	1962(12)	1224(7)	7016(7)		45(2)	27(5)	60(5)	34(5)	1(4)	1(4)	4(4)

Notes: Pb = non-split model. Pb' and Pb'' = split-model.

* U_{eq} defined as $\frac{1}{3}$ of the trace of the orthogonalized U_{ij} tensor.

† The anisotropic displacement exponent takes the form: $-2\pi^2(h^2a^2U_{11} + k^2b^2U_{22} + l^2c^2U_{33} + 2hka \cdot b \cdot U_{12} + 2hla \cdot c \cdot U_{13} + 2klb \cdot c \cdot U_{23})$.

TABLE 3. T-O bond lengths (Å)

T (°C)	20	230	465	700
T ₁ (0)-O _A (1)	1.642(7)	1.652(11)	1.647(11)	1.657(10)
T ₁ (0)-O _B (0)	1.630(7)	1.640(11)	1.625(13)	1.635(11)
T ₁ (0)-O _C (0)	1.624(6)	1.618(10)	1.621(10)	1.621(9)
T ₁ (0)-O _D (0)	1.641(7)	1.625(12)	1.613(13)	1.616(11)
Mean	1.634	1.634	1.627	1.632
T ₁ (z)-O _A (1)	1.748(7)	1.750(11)	1.755(11)	1.742(10)
T ₁ (z)-O _B (z)	1.716(7)	1.707(12)	1.713(12)	1.701(11)
T ₁ (z)-O _C (z)	1.721(6)	1.714(10)	1.708(10)	1.730(9)
T ₁ (z)-O _D (z)	1.747(7)	1.746(10)	1.748(11)	1.747(10)
Mean	1.733	1.729	1.731	1.730
T ₂ (0)-O _A (2)	1.732(5)	1.732(9)	1.731(10)	1.736(8)
T ₂ (0)-O _B (0)	1.707(7)	1.687(11)	1.701(13)	1.685(11)
T ₂ (0)-O _C (0)	1.706(7)	1.695(10)	1.739(12)	1.714(9)
T ₂ (0)-O _D (0)	1.712(7)	1.711(11)	1.708(13)	1.708(11)
Mean	1.714	1.706	1.720	1.711
T ₂ (z)-O _A (2)	1.632(6)	1.622(9)	1.625(9)	1.622(9)
T ₂ (z)-O _B (z)	1.603(7)	1.605(12)	1.620(12)	1.607(11)
T ₂ (z)-O _C (z)	1.620(7)	1.639(11)	1.582(11)	1.591(10)
T ₂ (z)-O _D (z)	1.630(7)	1.637(10)	1.642(10)	1.644(10)
Mean	1.621	1.626	1.617	1.616

in Tables 3 and 4. Table 5 contains the observed and calculated structure factors¹. A degree of Al-Si order (Q_{od}) of 0.71 was calculated on the room-temperature data, using the equation of Angel et al. (1990).

RESULTS AND DISCUSSION

Unit-cell parameters and structure evolution with temperature

The results obtained from the refinements show that: (1) the average T-O bond lengths and therefore the Al, Si site occupancies are not significantly changed at high temperature (Table 3). It must however be stressed that the large standard deviations on T and O atoms do not enable an accurate determination of the Q_{od} at HT. (2) The Fourier map near the Pb site shows a larger and more symmetrical electron density with increasing temperature (Fig. 1); the Fourier map has the same evolution with

¹ For a copy of Table 5, document item AM-98-002, contact the Business Office of the Mineralogical Society of America (see inside front cover of recent issue) for price information. Deposit items may also be available on the American Mineralogist web site at <http://www.minsocam.org>.

TABLE 4. Pb-O bond lengths (Å)

T (°C)	20	230	465	700
Pb-O _A (1)	2.748(7)	2.749(11)	2.760(11)	2.770(10)
Pb-O _A (1)	2.660(7)	2.690(11)	2.710(11)	2.733(10)
Pb-O _A (2)	2.493(6)	2.509(8)	2.514(8)	2.525(8)
Pb-O _B (0)	2.830(7)	2.845(11)	2.867(11)	2.904(10)
Pb-O _B (z)	3.079(7)	3.046(13)	3.010(13)	3.004(13)
Pb-O _C (0)	3.296(6)	3.274(10)	3.216(9)	3.220(9)
Pb-O _C (z)	3.025(6)	3.033(10)	3.091(10)	3.065(9)
Pb-O _D (0)	2.784(7)	2.828(11)	2.846(13)	2.843(11)
Pb-O _D (z)	2.626(7)	2.661(10)	2.699(11)	2.736(10)
< ^[6] Pb-O>	2.690	2.714	2.733	2.752
< ^[7] Pb-O>	2.738	2.759	2.772	2.788
< ^[9] Pb-O>	2.838	2.848	2.857	2.867

Note: The distances were calculated using the Pb coordinates from the Pb non-split model (Table 2).

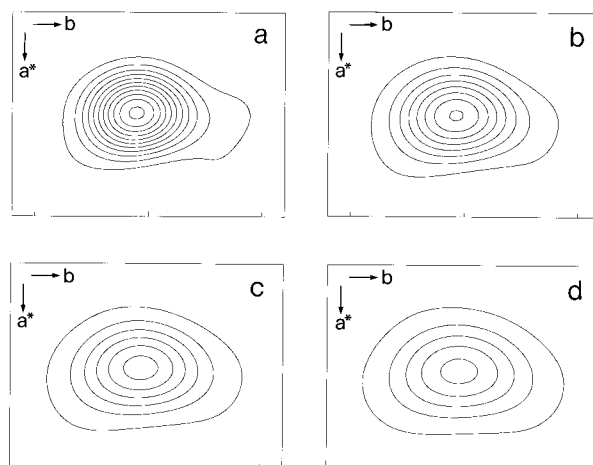


FIGURE 1. Electron-density maps for the Pb site viewed along the c axis; scale = 1 Å. (a) $T = 20$ °C; (b) $T = 230$ °C; (c) $T = 465$ °C; (d) $T = 700$ °C. Interval among contours is 30 $e^{-}/\text{Å}^3$. The coordinates of the center of the plots are: $x = 0.27$, $y = 0$, and $z = 0.07$.

temperature as was observed with decreasing Q_{od} in Tribaudino et al. (1998). (3) With increasing temperature the average position of the Pb atom moves significantly toward the glide plane (i.e., $y/b = 0$) (Fig. 2). (4) The Pb-O distances undergo a significant increase with temperature (Table 4). It appears that the bond lengths between Pb and O atoms that are pseudosymmetric in $I2/c$ become progressively similar to one another (Fig. 3). This is mainly due to the shift of Pb toward the glide plane as

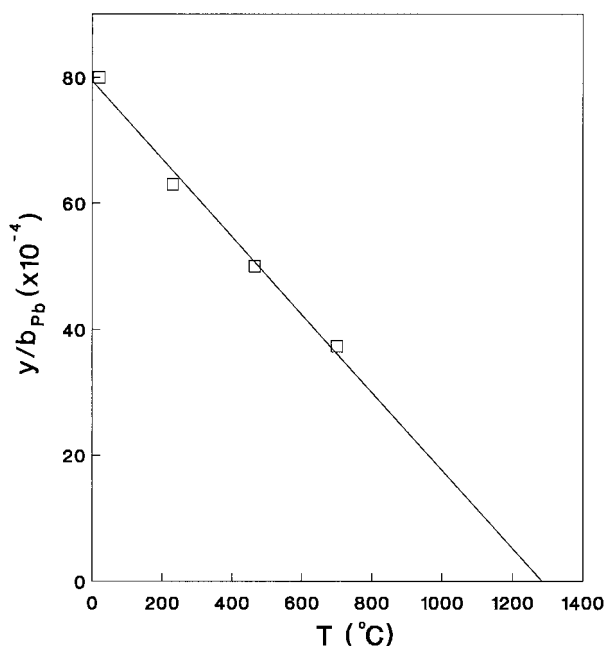


FIGURE 2. Absolute value of y/b fractional coordinate of the Pb site vs. T .

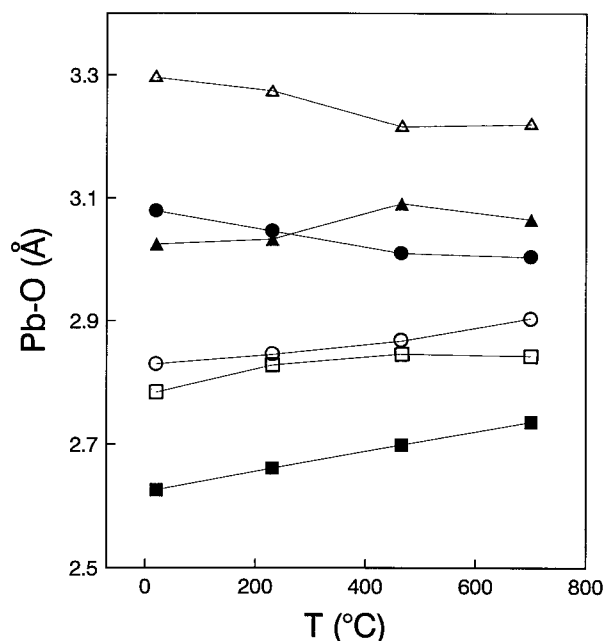


FIGURE 3. Pb-O distances vs. T for pseudosymmetrical O atoms. Circles = OB; triangles = OC; squares = OD. Open symbol = 0; full symbol = z.

the distance of the split vector of pseudosymmetric atoms does not significantly reduce.

The thermal expansion of the unit-cell parameters follows the trend observed in monoclinic feldspars (Oehlschlegel et al. 1974; Henderson and Ellis 1976; Henderson 1984). The main expansion is observed along the a direction, with a slight decrease of the β angle, whereas the expansion along b and c is rather small. The overall volume expansion is $1.26 \times 10^{-5} \text{ }^\circ\text{C}^{-1}$ for the investigated sample, and is close to that observed for strontium, barium and calcium feldspars (1.35, 1.15, and $0.88 \times 10^{-5} \text{ }^\circ\text{C}^{-1}$, Henderson 1984). The volume expansion is lower in feldspars with divalent cation than in alkali feldspars, mainly due to a lower expansion along a . The thermal expansion ellipsoid, calculated as in Ohashi (1982), shows that in lead feldspar the main expansion occurs along a direction close to a^* (Table 6), as in all monoclinic feldspars.

In Figure 4 the main structural features along a^* in lead feldspar are considered. The OA2-OA2 distance along the Pb polyhedron (AB) and the OA2-OA2 distance along the tetrahedral cage (BC) are shown. In the Pb polyhedron the Pb-OA2 distance expands significantly. The expansion of the Pb-Pb distance, together with the Pb-OA2 distance, accounts for the overall increase of the distance between the two OA2 atoms along the Pb polyhedron (AB). The above increase would be significantly higher than the actual cell expansion along a^* . In fact, the size of the tetrahedral cage along a^* (BC) decreases with increasing temperature, thus partially compensating the expansion of the polyhedron. The mechanism of ex-

TABLE 6. Principal axes of the strain ellipsoid (20–700 $^\circ\text{C}$)

	Strain ($\times 10^{-3}$)	Angle with		
		a	b	c
ϵ_1	5.9(3)	19	90	96
ϵ_2	1.6(3)	109	90	6
ϵ_3	1.1(2)	90	0	90

Note: The reference state is at $T = 20 \text{ }^\circ\text{C}$.

pansion with temperature in lead feldspar (Fig. 5a) is the same as in sanidine (Fig. 5b) (Ohashi and Finger 1974, 1975), but the absolute value of partial contributions of the tetrahedral cage and of the M polyhedron are higher in sanidine than in lead feldspar and an higher expansion along a^* is observed in sanidine. This probably results as an effect of the stronger bonding of the divalent lead cation with O atoms in comparison with potassium.

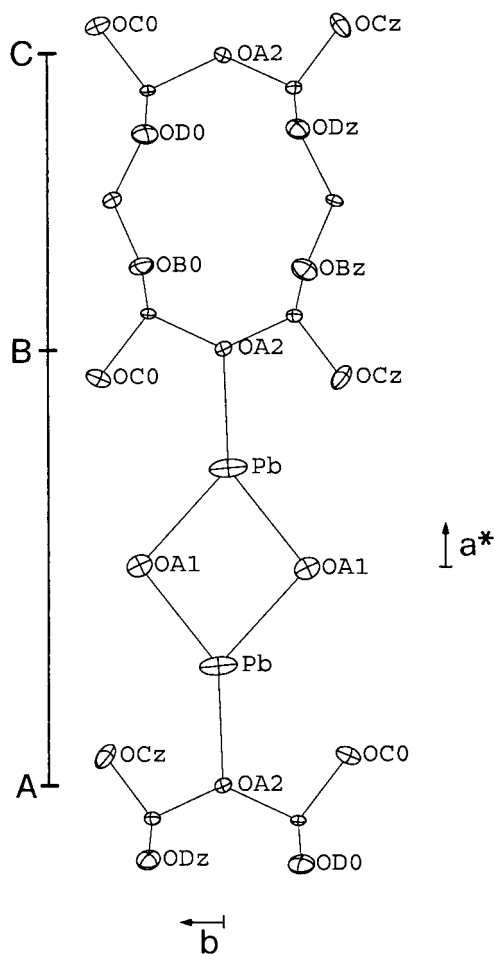


FIGURE 4. Partial projection along the c axis of the lead feldspar structure. T atoms are not labeled. AB = OA2-OA2 distance along the Pb polyhedron; BC = OA2-OA2 distance along the tetrahedral cage.

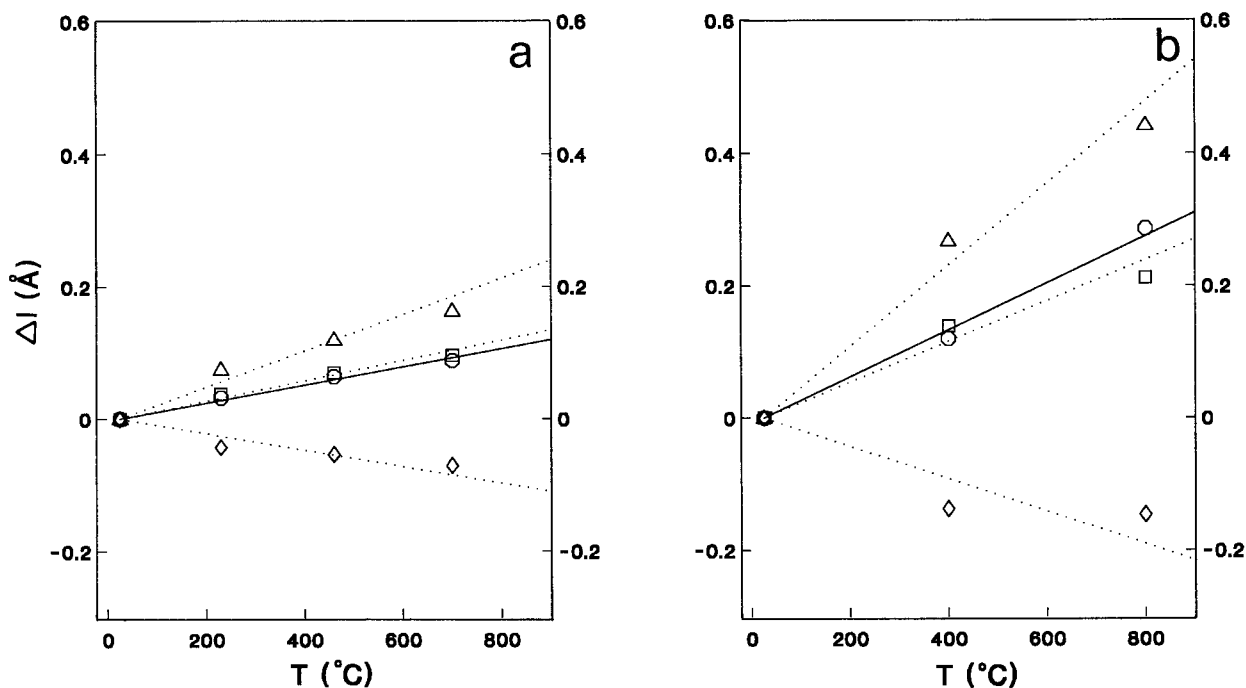


FIGURE 5. Differences of the main interatomic distances along a^* (Δl) in comparison with the 20 °C values vs. T for (a) lead feldspar and (b) sanidine (Ohashi and Finger 1974, 1975). Triangles = OA2-OA2 distance along the M polyhedron; squares = M-M distance; diamonds = OA2-OA2 distance along the tetrahedral cage (dotted line). Circles = $2 \times d_{100}$ distance (full line).

Evolution of b -type reflections with temperature

Tribaudino et al. (1998) observed that the intensity of the b -type superstructure reflections arises in monoclinic $I2/c$ feldspars both from Al-Si ordering (i.e., framework contribution) and from the displacement of the non-tetrahedral cation away from the glide plane (cation contribution). The cation contribution in lead feldspar is significantly higher than the framework contribution when it is monitored by X-ray, due to the very strong scattering power of lead. Indeed, the strong decrease in the b reflections intensity with Al-Si disorder was mainly due to the related approach of the average coordinate of Pb to the glide plane.

Increasing temperature induces a significant decrease in the intensity of the b reflections compared to the intensity of a -type reflections (Table 1). The evolution of the intensity of the b reflections with temperature is affected by several factors. As shown above, both cation and framework contribution may change their intensity; moreover a decrease in the intensity, affecting also a reflections, comes from the increased atomic displacements parameters (ADP) observed at HT. Following Foit and Peacor (1973), the structure factors for the most intense b reflections were separately calculated for T and O atoms (framework contribution) and for Pb atom (Pb contribution) using positional and displacement parameters from the refinement at $T = 20$ °C (Table 7). The framework contribution (F_{frame}) was calculated considering a fictive structure with Pb placed onto the glide plane and T and O atoms fixed as in the 20 °C refinement. The Pb contribution (F_{Pb}) was instead calculated in a $I2/c$ model where T and O sites, equivalent in $C2/m$ space group, were fixed in an averaged intermediate position and Pb was left in the room temperature position ($y/b = -0.008$). From Table 7, in most reflections, the Pb contribution accounts almost completely to the value of the calculated structure factors.

TABLE 7. Calculated framework and Pb contribution to structure factors compared with the F_c values obtained in the refinement for some b reflections

b refl.	F_{frame}	F_{Pb}	$F_{\text{frame}} + F_{\text{Pb}}$	F_c (refinement)
$\bar{1} 2 1$	-15.5	-58.4	-73.9	-71.2
0 3 1	15.3	42.5	57.8	52.0
1 4 1	-1.3	81.5	80.2	77.9
0 5 1	1.2	50.2	51.4	51.6
1 6 1	9.6	96.7	106.3	104.8
0 7 1	-0.1	50.3	50.2	54.4
1 8 1	-7.6	96.1	88.5	88.4
0 11 1	10.3	47.0	57.3	53.8
$\bar{2} 1 3$	-13.2	-25.8	-39.0	-37.3
0 5 3	5.6	106.5	112.7	110.0
$\bar{4} 7 3$	4.1	69.6	73.7	73.4
0 9 3	-0.5	109.4	108.9	107.5
1 4 5	2.2	-63.7	-61.5	-60.1
0 5 5	11.0	70.6	81.6	81.1
1 6 5	1.3	-75.3	-74.0	-75.4
$\bar{2} 7 5$	-18.0	-96.7	-114.7	-115.3
0 9 5	16.2	72.7	88.9	90.4

In Figure 6 the evolution of the calculated structure factors of the b reflections 161 and 093 is shown vs. the

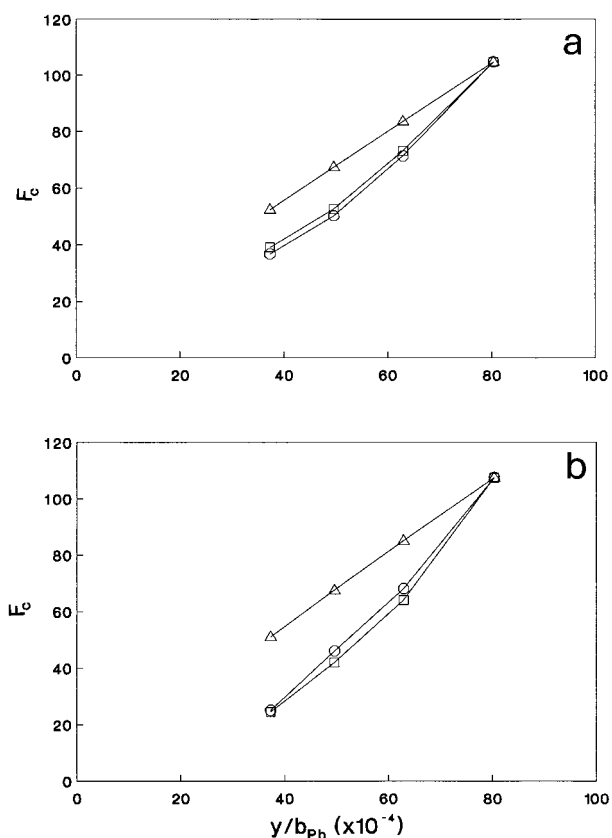


FIGURE 6. Calculated structure factors (F_c) vs. y/b fractional coordinate of the Pb site for the b reflections 161 (a) and 093 (b). Model 1 (triangles) = coordinates of Pb at the different T ; ADP of Pb, coordinates, and ADP of framework atoms at $T = 20$ °C. Model 2 (squares) = coordinates and ADP of Pb at the different T ; coordinates and ADP of framework atoms at $T = 20$ °C. Model 3 (circles) = actual refinements at different T .

shift away from the plane of the Pb atom, observed at different temperatures. Three models were reported starting from the F_c obtained at 20 °C ($y/b_{Pb} = -0.008$). In the first model the coordinates of Pb retained the values obtained at the different temperatures, whereas the ADP of Pb and the coordinates and the ADP of the framework atoms were fixed to the values obtained at 20 °C. In the second model both the coordinates and the ADP of Pb had the refined value for each temperature, whereas the framework atoms had the coordinates and ADP fixed to the 20 °C value. In the third model the actual values of coordinates and of ADP for all the atoms were used for the calculation. The striking similarity of the second model with the third model results (actual refinements) shows that the reduction with temperature of the b reflection intensity is almost completely due to changes in the positional and atomic displacement parameters of Pb. This behavior is observed in most of the b reflections.

The low contribution of the framework to the b reflections makes it difficult to evaluate any possible change of the order parameter (Q_{od}) with temperature. This is a

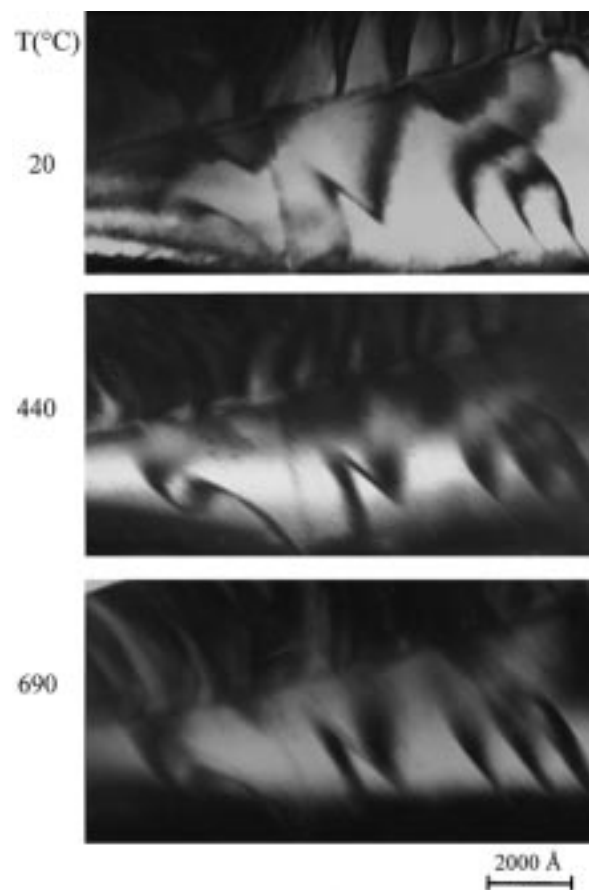


FIGURE 7. Dark field images of b antiphase domains in PbF at different T ; $g = 031$.

problem at HT where the enlargement of thermal parameters further decreases the b reflections intensity. The direct measurement of Q_{od} at HT is therefore questionable. However some evidence exists that Q_{od} did not change significantly during the HT collection. A change in Q_{od} was observed only after thermal treatment at temperatures higher than the experimental conditions of this work ($T > 850$ °C, Tribaudino et al. 1998) or in long duration hydrothermal runs (Bruno and Facchinelli 1972); moreover a data collection and refinement was performed on the sample at room temperature after the heating run, with no significant change concerning Q_{od} in comparison with the results obtained before heating.

In situ TEM observation up to about 690 °C (Fig. 7) did not show changes in size and shape in the b antiphase domains, neither did a diffuse component appear in the relevant diffraction patterns up to 935 °C (Fig. 8). It can therefore be assumed that the change of the Pb configuration, does not change the domain structure of the feldspar; this instead seems mainly related to the Al-Si ordering, which is assumed constant within the examined temperature range.

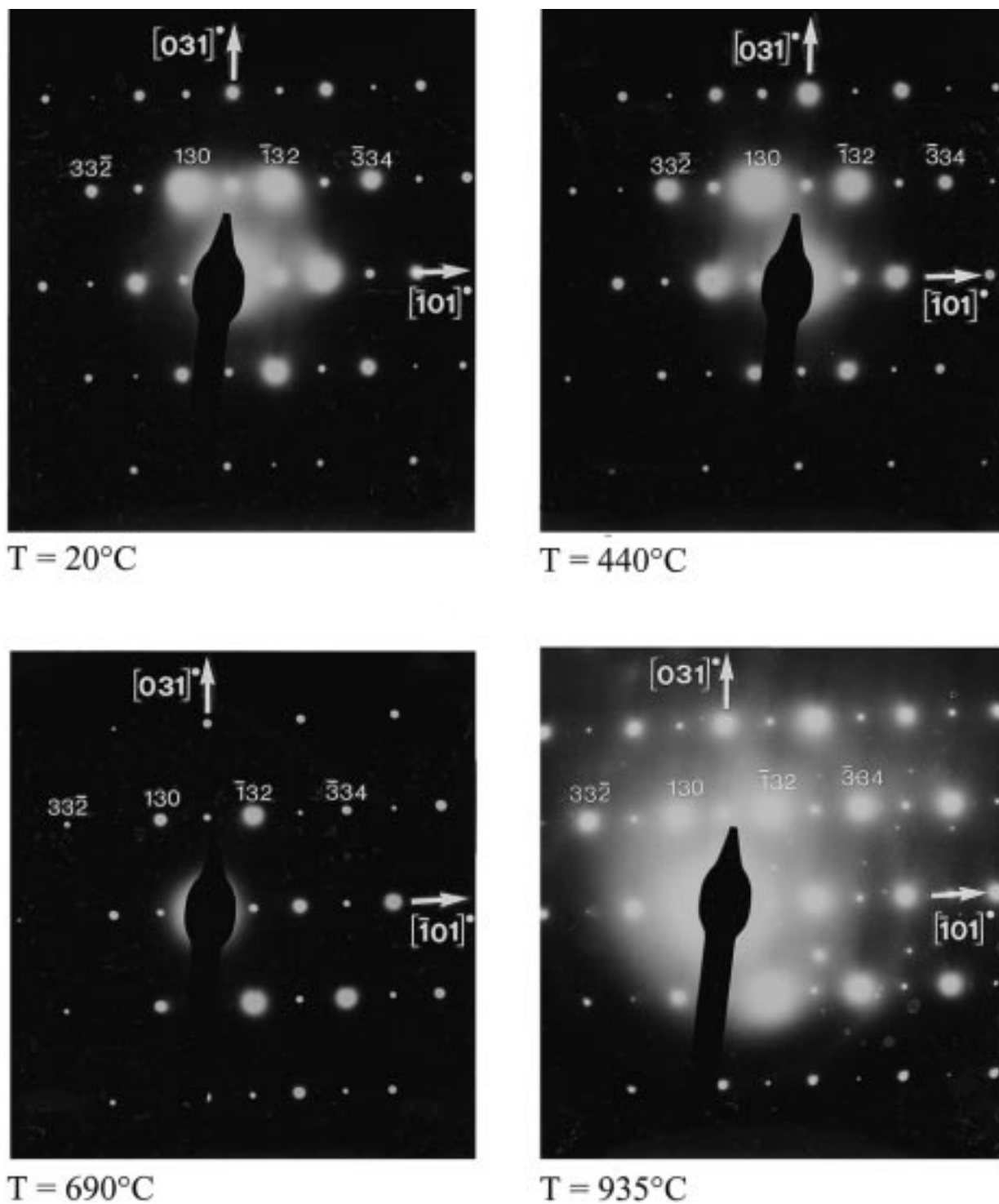


FIGURE 8. SAD pattern of PbF along $[3\bar{1}\bar{3}]$ at different T . Both a and b type reflections are present.

Displacement parameters and lead electron-density

Previously the electron-density distribution observed around the Pb site was assumed to be an effect of positional disorder, rather than due to dynamical effects. The vibrational component of the displacement parameters, at

a temperature sufficiently high that the zero-point motion effects are negligible, is expected to increase linearly with temperature, with an intercept at $T = 0$ K that goes through the origin if the vibration is only due to a thermal motion component. If the displacement parameters are af-

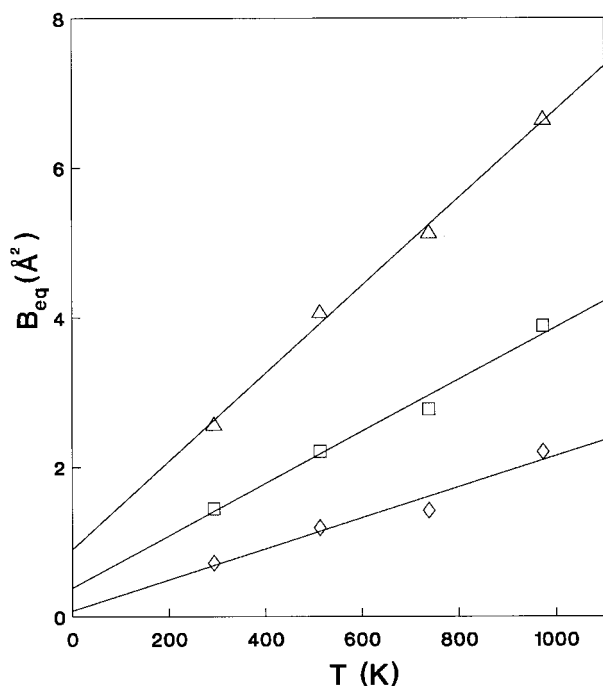


FIGURE 9. Equivalent isotropic displacement factors B_{eq} vs. T . Triangles = Pb; squares = O atoms; diamonds = T atoms.

ected also by positional disorder a significant intercept at 0 K is instead expected (Smith et al. 1986; Pavese et al. 1995). The temperature at which the zero-point motion is no longer negligible cannot be simply predicted in the absence of low temperature refinements, although previous refinements for low albite (Smith et al. 1986) suggest that in feldspar the zero-point contribution is not significant at least down to room temperature.

In Figure 9 the evolution with temperature of the equivalent displacement parameters in the refined sample are given for Pb and for an average of O and T atoms. The "non-split model" was used for Pb. An extrapolation to $T = 0$ K for the higher temperature data shows the presence of a significant residual for the Pb and for O atoms [respectively, $B_{eq} = 0.94(23)$ and $0.40(21)$ \AA^2] thus indicating the presence of positional disorder. The 0 K intercept does not result in a significant residual for the T atoms [$B_{eq} = 0.09(21)$ \AA^2]. This suggests that positional disorder in Pb induces a significant disorder in the O atoms, which are nearest neighbors with Pb, but not in T atoms that are coordinated by O atoms.

The evolution of the electron-density distribution around the Pb site with temperature (Fig. 1) shows a remarkable similarity to that observed for increasing Al-Si disorder: at low temperature a tail is observed in the electron-density, which increases with temperature, whereas the 700 °C electron-density map is not far from the bean-like appearance found in the most disordered samples at room temperature (Tribaudino et al. 1998). The HT configuration is induced by increased thermal vibration, at constant Q_{od} , whereas the electron-density observed at

room temperature in samples with high Al-Si disorder is interpreted as induced by increased static positional disorder of the Pb atom, that occurs as a consequence of varying local Al-Si configurations (Benna et al. 1996). The presence of a smeared electron-density and the approach to the glide plane of the average position of Pb are observed both with increased Al-Si disorder and at HT. As a consequence, the intensity of the b reflections reduces dramatically, despite the apparent lack of significant Al-Si disordering at the investigated temperatures.

The approach of the average coordinate of Pb to the glide plane is linear with temperature in the investigated range (Fig. 2). If the approach is still linear at higher temperatures, at $T \sim 1300$ °C the Pb lies on the glide plane. This temperature is not far from that found for the $C2/m-I2/c$ phase transition (1180 °C, Tribaudino et al. 1998). It appears therefore that at a temperature close to the transition Pb assumes, at constant Q_{od} , the same position and the same electron-density distribution which is observed at room temperature in the disordered sample. The average Pb position on the m plane would be that present in $C2/m$ symmetry, in a configuration obviously more regular than the $I2/c$ configuration at room temperature (Benna et al. 1996). This suggests that at HT the Pb atom has a configuration that may favor Al-Si disorder.

ACKNOWLEDGMENTS

We thank Simon A. T. Redfern for critical reading and useful suggestions. Reviews from Michael A. Carpenter and Thomas Malcherek greatly improved the manuscript. This work was supported by M.U.R.S.T.—Project "Relations between structure and properties in minerals: analysis and applications," Roma, and by C.S. Geodinamica Catene Collisionali CNR, Torino.

REFERENCES CITED

- Angel, R.J., Carpenter, M.A., and Finger, L.W. (1990) Structural variation associated with compositional variation and order-disorder behavior in anorthite-rich feldspar. *American Mineralogist*, 75, 150–162.
- Argoud, R. and Capponi, J.J. (1984) Soufflette à haute température pour l'étude de monocristaux aux rayons X et aux neutrons jusqu'à 1400 K. *Journal of Applied Crystallography*, 17, 420–425.
- Benna, P., Zanini, G., and Bruno, E. (1985) Cell parameters of thermally treated anorthite. Al, Si configurations in the average structures of the high temperature calcic plagioclases. *Contributions to Mineralogy and Petrology*, 90, 381–385.
- Benna, P., Tribaudino, M., and Bruno, E. (1995) Al-Si ordering in Sr-feldspar $\text{SrAl}_2\text{Si}_2\text{O}_8$: IR, TEM and single-crystal XRD evidences. *Physics and Chemistry of Minerals*, 22, 343–350.
- (1996) The structure of ordered and disordered lead feldspar ($\text{PbAl}_2\text{Si}_2\text{O}_8$). *American Mineralogist*, 81, 1337–1343.
- Bruno, E. and Facchinelli, A. (1972) Al, Si configurations in lead feldspar. *Zeitschrift für Kristallographie*, 136, 296–304.
- Carpenter, M.A. (1992) Equilibrium thermodynamics of Al/Si ordering in anorthite. *Physics and Chemistry of Minerals*, 19, 1–24.
- Czank, M. (1973) Strukturuntersuchungen von Anorthit im Temperaturbereich von 20°C bis 1430°C. Dissertation. ETH, Zürich.
- Foit, F.F. and Peacor, J.R. (1973) The anorthite crystal structure at 410 and 830 °C. *American Mineralogist*, 58, 665–675.
- Ghose, S., McMullan, R.K., and Weber, H.P. (1993) Neutron diffraction studies of the $P1-I1$ transition in anorthite ($\text{CaAl}_2\text{Si}_2\text{O}_8$), and the crystal structure of the body-centered phase at 514K. *Zeitschrift für Kristallographie*, 204, 215–237.
- Henderson, C.M.B. (1984) Thermal expansion of feldspars III. Rb-

- GaSi₃O₈-sanidine, Sr-feldspar and an ordered microcline-albite solid solution (Or_{62.4} mole%). *Natural Environment Research Council, Progress in Experimental Petrology*, 25, 78–83. Cambridge University Press, Cambridge, U.K.
- Henderson, C.M.B. and Ellis, J. (1976) Thermal expansion of synthetic alkali feldspars. *Natural Environment Research Council, Progress in Experimental Petrology*, 55–59. Constable Ltd., Edinburgh, U.K.
- Kimata, M., Shimizu, M., and Saito, S. (1996) High-temperature crystal structure of sanidine. Part II: The crystal structure of sanidine at 935°C. *European Journal of Mineralogy*, 8, 15–24.
- Malcherek, T., Kroll H., Schleiter, M., and Salje, E.K.H. (1995) The kinetics of the monoclinic to monoclinic phase transition in BaAl₂Ge₂O₈-feldspar. *Phase Transitions*, 55, 199–215.
- North, A.C.T., Phillips, D.C., and Mathews, F.S. (1968) A semi-empirical method of absorption correction. *Acta Crystallographica*, A24, 351–359.
- Oehlschlegel, G., Kockel, A., and Biedl, A. (1974) Anisotrope Wärmedehnung und Mischkristallbildung einiger Verbindungen des ternären Systems BaO-Al₂O₃-SiO₂, II. Messungen an Strukturen mit dreidimensionaler Verknüpfung von (Si,Al)O₄-tetraedern und Modellvorstellungen über deren Wärmedehnungsanisotropie. *Glastechnische Berichte*, 47, 31–41.
- Ohashi, Y. (1982) A program to calculate the strain tensor from two sets of unit-cell parameters. In R.M. Hazen and L.W. Finger, Eds., *Comparative crystal chemistry*, p. 92–102. Wiley, Chichester, U.K.
- Ohashi, Y. and Finger, L.W. (1974) Refinement of the crystal structure of sanidine at 25° and 400°C. *Carnegie Institution of Washington Year Book*, 73, 539–544.
- (1975) An effect of temperature on the feldspar structure: crystal structure of sanidine at 800°C. *Carnegie Institution of Washington Year Book*, 74, 569–572.
- Pavese, A., Artioli, G., and Prencipe, M. (1995) X-ray single crystal diffraction study of pyrope in the temperature range 30–973 K. *American Mineralogist*, 80, 457–464.
- Prewitt, C.T., Sueno, S., and Papike, J.J. (1976) The crystal structures of high albite and monalbite at high temperatures. *American Mineralogist*, 61, 1213–1225.
- Ribbe, P.H. (1994) The crystal structures of the aluminum-silicate feldspars. In I. Parsons, Ed., *Feldspars and their reactions*, p. 1–49. Kluwer, Dordrecht.
- Smith, J.V., Artioli, G., and Kvik, Å. (1986) Low albite, NaAlSi₃O₈: neutron diffraction study of crystal structure at 13K. *American Mineralogist*, 71, 727–733.
- Tribaudino, M., Benna, P., and Bruno, E. (1998) Structural variations induced by thermal treatment in lead feldspar (PbAl₂Si₂O₈). *American Mineralogist*, 83, 159–166.
- Winter, J.K., Ghose, S., and Okamura, F.P. (1977) A high-temperature study of the thermal expansion and the anisotropy of the sodium atom in low albite. *American Mineralogist*, 62, 921–931.

MANUSCRIPT RECEIVED MAY 15, 1998

MANUSCRIPT ACCEPTED SEPTEMBER 7, 1998

PAPER HANDLED BY SIMON A.T. REDFERN